Journal of Power Sources 252 (2014) 73–78

Contents lists available at ScienceDirect

Journal of Power Sources

journal homepage: www.elsevier.com/locate/jpowsour

Short communication

Improvement of electrochemical performance for spherical $LiFePO_4$ via hybrid coated with electron conductive carbon and fast Li ion conductive $La_{0.56}Li_{0.33}TiO_3$

Hongbo Shu, Manfang Chen, Yanqing Fu, Xiukang Yang, Xin Yi, Yansong Bai, Qianqian Liang, Qiliang Wei, Benan Hu, Jinli Tan, Chun Wu, Meng Zhou, Xianyou Wang*

Key Laboratory of Environmentally Friendly Chemistry and Applications of Ministry of Education, School of Chemistry, Xiangtan University, Hunan, Xiangtan 411105, China

HIGHLIGHTS

- Spherical $LiFePO_4/(C + La_{0.56}Li_{0.33}TiO_3)$ composites are firstly reported.
- The hybrid coating layer was uniformly deposited on the surface of $LiFePO_4$.
- The hybrid coating layer can be favourable for fast electron and Li^+ transport.
- The performance of $LiFePO_4/C$ is improved via coating with $La_{0.56}Li_{0.33}TiO_3$.
- This strategy can be extended to other materials for lithium ion batteries.

ARTICLE INFO

Article history:
Received 2 July 2013
Received in revised form
30 October 2013
Accepted 17 November 2013
Available online 26 November 2013

Keywords:
Lithium ion batteries
Spherical lithium iron phosphate
Fast Li ion conductor
Hybrid coating
Electrochemical performance

ABSTRACT

The $LiFePO_4/(C + La_{0.56}Li_{0.33}TiO_3)$ composites with spherical morphology are synthesized for the first time via ammonia assisted hydrothermal method. The structure and electrochemical performance of $LiFePO_4/(C + La_{0.56}Li_{0.33}TiO_3)$ are investigated by scanning electron microscope (SEM), transmission electron microscopy (TEM), X-ray diffraction (XRD), charge/discharge tests and cyclic voltammetry (CV). It has been found that the hybrid coating layer composing of electron conductive C and fast Li ion conductive $La_{0.56}Li_{0.33}TiO_3$ is synchronously deposited on the surface of $LiFePO_4$ microspheres. The hybrid coating layer can be favourable for fast electron and Li^+ transport, and avoid HF eroding $LiFePO_4$ in electrolyte, thus improve the electrochemical performance. The initial discharge capacity of $LiFePO_4/(C + La_{0.56}Li_{0.33}TiO_3)$ is 126.3 mAh g^{-1}, the capacity retention is still as high as 98.3% even after 100 cycles at 5 C. Even at high rate of 30 C, it still reveals a high discharge capacity of 62.3 mAh g^{-1}.

1. Introduction

Since the pioneering work by Padhi [1], the olivine $LiFePO_4$ has been regarded as the most promising candidate of cathode materials for lithium ion batteries because of its high theoretical capacity, long cycle life, good thermal stability, excellent safety and so on [2]. Unfortunately, the low tap density (~0.9 g cm^{-3}), poor electronic conductivity (10^{-9} to 10^{-8} S cm^{-1}), low ionic conductivity (10^{-11}–10^{-9} S cm^{-1}) and low ionic diffusivity (10^{-17}–10^{-14} cm^2 s^{-1}) have hampered its extensive applications in industry [3,4].

Extensive works have been introduced to overcome intrinsic shortcomings of $LiFePO_4$. One way is to synthesize spherical morphology material with high tap density [5–8]. Another important approach is surface coating of $LiFePO_4$ with electronic conductive materials (such as carbon, polymers and so on) to enhance electronic conductivity of $LiFePO_4$ [9–16]. While transferred electron in $LiFePO_4$ must be reciprocally compensated by extraction/insertion of Li^+ to keep the charge balance during the charging/discharging process [2]. If the Li ion diffusivity cannot attain the requisite diffusivity of transferred electron, it will limit the transferred electron, leading to deteriorated electrochemical performance. Thus, it is necessary to seek for an ideal coating layer with both high Li^+ and electron conductivity.

$La_{0.56}Li_{0.33}TiO_3$ with a perovskite structure is an excellent fast Li ion conductor [17–20]. The lithium ion conductivity of

* Corresponding author. Tel.: +86 731 58292060; fax: +86 731 58292061.
E-mail address: wxianyou@yahoo.com (X. Wang).

0378-7753/$ – see front matter
http://dx.doi.org/10.1016/j.jpowsour.2013.11.036

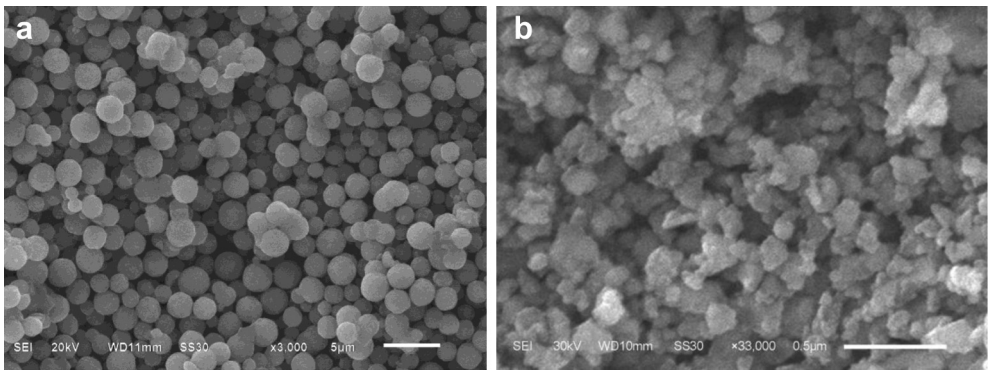

Fig. 1. SEM images of the synthesized (a) $LiFePO_4$ precursor and (b) $La_{0.56}Li_{0.33}TiO_3$.

$La_{0.56}Li_{0.33}TiO_3$ is up to 10^{-3} S cm^{-1} at 25 °C, and gradually enhances with the increase of temperature. Moreover, it exhibits a good thermal stability, low cost and excellent safety [17–20]. Therefore, it has extensively been used in electrolyte of batteries and other electrochemical devices [17–20]. To our knowledge, there have been rarely reports on using $La_{0.56}Li_{0.33}TiO_3$ or $La_{0.56}Li_{0.33}TiO_3$ and C hybrid coating to modify $LiFePO_4$.

Recently, we have successfully synthesized $LiFePO_4$/C microspheres via ammonia assisted hydrothermal route and achieved excellent electrochemical performance [6–8]. In order to further improve the electrical properties of $LiFePO_4$/C, especially high rate capability, herein we reported $LiFePO_4$/(C + $La_{0.56}Li_{0.33}TiO_3$) microspheres modified with electron conductive C and fast Li ion conductive $La_{0.56}Li_{0.33}TiO_3$ hybrid coating.

2. Experimental

Nano-powders $La_{0.56}Li_{0.33}TiO_3$ was synthesized by sol–gel method as follows. Separately, the stoichiometric amounts of 0.03 mol of citric acid, $Ti(OBu)_4$, $La(NO_3)_3 \cdot 6H_2O$ and $LiNO_3$ (mole ratio is 1.15:1.00:0.56:0.33) was dissolved in 150 mL ethanol with stirring at room temperature. Then the solution was heated on a hotplate at 80 °C under continued stirring to get gel. The obtained gel was placed into an oven at 80 °C to form xerogel. The xerogel were ground and preheated at 350 °C for 4 h. After cooled to room temperature, the obtained precursor were ground again and then calcined at 900 °C for 2 h. Finally, the $La_{0.56}Li_{0.33}TiO_3$ was obtained.

$LiFePO_4$/(C + $La_{0.56}Li_{0.33}TiO_3$) composites were prepared as follows. The stoichiometric amounts of 0.028 mol of $LiOH \cdot H_2O$,

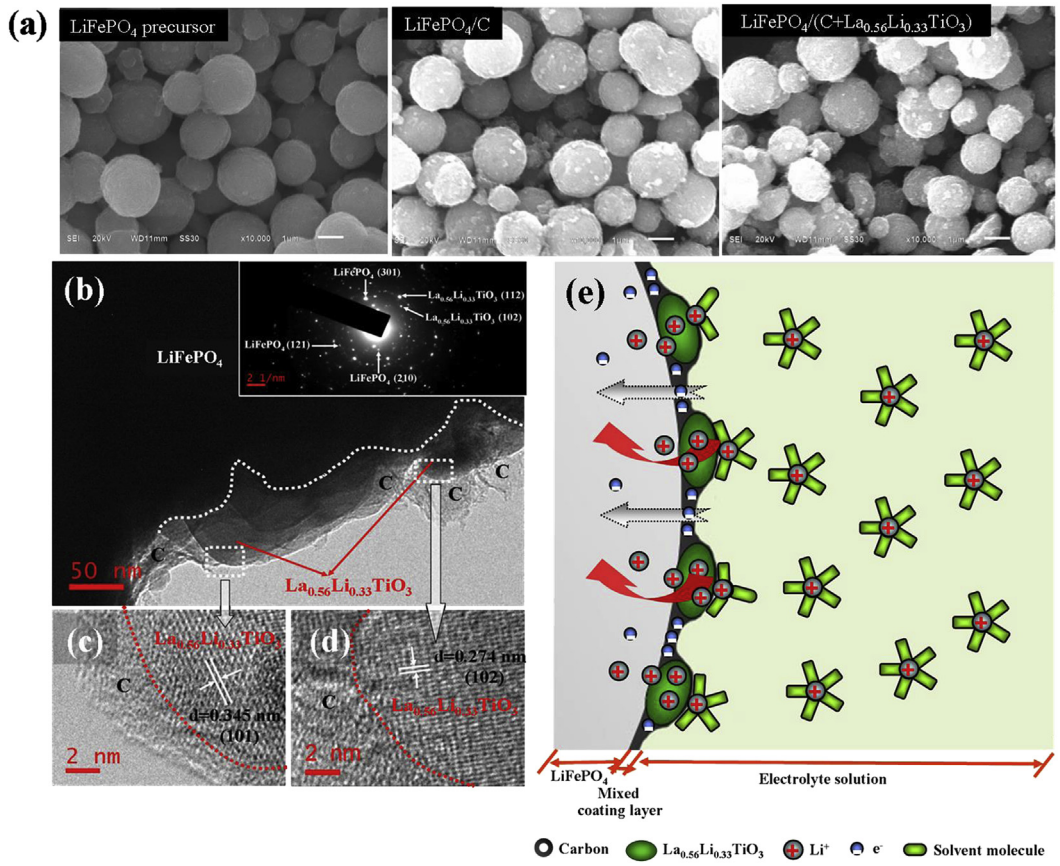

Fig. 2. (a) SEM images of the synthesized samples; (b) TEM and (c, d) HR-TEM (inset: SAED) photograph of synthesized $LiFePO_4$/(C + $La_{0.56}Li_{0.33}TiO_3$); (e) Schematic of the hybrid coating layer with C and $La_{0.56}Li_{0.33}TiO_3$ for $LiFePO_4$ during charge/discharge process.

$Fe(NO_3)_3 \cdot 9H_2O$, $NH_4H_2PO_4$ and citric acid with molar ratio of 1:1:1:1 were dissolved in 45 mL distilled water to form a transparent yellow-green solution. Then 2 mL ammonia solution (25%–28% *V*%) was dropwise added to the solution with continued stirring. A certain amount of distilled water was added to above solution up to 70 mL. The mixture solution was stirred for 30 min before being transferred into a 100 mL Teflon-lined stainless steel autoclave. The autoclave was sealed, kept at 180 °C for 6 h in an electric oven, and cooled to room temperature naturally. The suspension and precipitate were heated on a hotplate at 80 °C under stirring to get spherical precursor powder. The spherical precursor powder was directly mixed with $La_{0.56}Li_{0.33}TiO_3$ (about 2 wt.% of $LiFePO_4$) and solid citric acid (the amount of carbon was about 5 wt.% of $LiFePO_4$) in ethanol medium. The powder was calcined at 700 °C for 10 h in Ar/H_2 (95:5 V%) atmosphere. Finally, $LiFePO_4$/(C + $La_{0.56}Li_{0.33}TiO_3$) composites were obtained. For comparison, $LiFePO_4$/C composites were prepared by the above process without $La_{0.56}Li_{0.33}TiO_3$.

The phase identification of the samples was performed with a diffractometer (D/Max-3C, Rigaku, Japan) using Cu Kα radiation ($\lambda = 1.54178$ Å) and a graphite monochromator at 36 kV, 20 mA. The surface morphology of the samples was observed using the JSM-6100LV SEM (JEOL, Japan) equipped with an energy dispersive spectrometer (EDS). High resolution transmission electron microscopy (HR-TEM) and selected area electron diffraction (SAED) images were taken with JEOL JEM100SX electron microscope. The weight percentage of carbon in the samples was determined by a C, H, N Analyser model 1106 Carlo Erba Strumentazione. The measured volume of the tapped powder and its mass were used to calculate the tap density of $LiFePO_4$/C.

The electrochemical tests of samples were carried out using coin cells assembled in an argon-filled glove box. In all cells, the cathode was consisted of a mixture of active material (80 wt.%), acetylene black (5 wt.%), graphite (5 wt.%) and polyvinylidene fluoride (PVDF) (10 wt.%); lithium was served as counter and reference electrodes; a Celgard 2400 was used as separator, and the electrolyte was 1 M $LiPF_6$ solution in ethylene carbonate (EC)-dimethyl carbonate (DMC) (1:1, V/V). The loading of samples on the electrode is about 9.5 mg cm^{-2}, and the thin film of electrode is around 75 μm in thickness after rolling. Charge/discharge measurement was carried out in Neware battery test system BTS-XWJ-6.44S-00052 at different current densities between 2.0 and 4.3 V vs. Li/Li^+. CV was performed on Zahner Zennium electrochemical workstation in the potential ranges of 2.0–4.3 V (vs. Li/Li^+) at room temperature at the scan rates from 0.1 to 1.0 mV s^{-1}.

3. Results and discussion

SEM images of synthesized samples are shown in Fig. 1. $LiFePO_4$ precursor is uniform monodisperse microspheres with the average particle size of about 1.8 μm $La_{0.56}Li_{0.33}TiO_3$ is composed of near-spherical nanoparticles with the particle size of about 30–200 nm. $LiFePO_4$/(C + $La_{0.56}Li_{0.33}TiO_3$) composites is obtained via solid state reaction.

The morphologies of as-synthesized samples are shown in Fig. 2a. It can be clearly seen that $LiFePO_4$/C and $LiFePO_4$/(C + $La_{0.56}Li_{0.33}TiO_3$) exhibit nearly the same shape and size as precursor, even after the precursor re-crystallized under the high temperature calcination. The tap density of both synthesized samples is around 1.3 g cm^{-3}. The surface morphology of $LiFePO_4$/(C + $La_{0.56}Li_{0.33}TiO_3$) is investigated by TEM and HR-TEM shown in Fig. 2b–d. As illustrated in Fig. 2b, there are two distinctive morphologies, namely relatively dark nanoparticles and grey floccule deposited on the surface of $LiFePO_4$ particles. Fig. 2c–d show the HR-TEM of these two materials. The relatively dark nanoparticles are crystalline $La_{0.56}Li_{0.33}TiO_3$ and the grey floccule is amorphous carbon, respectively. The residual carbon content is about 4.1 wt.%, determined by element analysis. The SAED patterns shown in the inset of Fig. 2b further reveal the existence of high crystallinity $La_{0.56}Li_{0.33}TiO_3$ in the hybrid coating layer. Basing on the above results, it indicates that C as an excellent electronic conductor and $La_{0.56}Li_{0.33}TiO_3$ as a perfect fast Li ion conductor are synchronously coated on the surface of spherical $LiFePO_4$. The hybrid coating layer is not only favourable to fast transport both electron and Li^+, but also prevents direct contact between electrolyte and $LiFePO_4$, and thus could improves the electrochemical performance, especially high rate capability and cyclic stability. A schematic drawing of this is exhibited in Fig. 2e.

The XRD patterns of synthesized $La_{0.56}Li_{0.33}TiO_3$, $LiFePO_4$/C and $LiFePO_4$/(C + $La_{0.56}Li_{0.33}TiO_3$) are displayed in Fig. 3a. The results show that synthesized $La_{0.56}Li_{0.33}TiO_3$ can be indexed as perovskite structure, indicating a perfect crystallinity [17–20]. It is also worth mentioning that the synthesized $LiFePO_4$/C and $LiFePO_4$/(C + $La_{0.56}Li_{0.33}TiO_3$) still retain the olivine $LiFePO_4$ after coating with C and $La_{0.56}Li_{0.33}TiO_3$, as corroborated by the XRD patterns results shown in Fig. 3a. In addition, the chemical valences of Ti for $LiFePO_4$/(C + $La_{0.56}Li_{0.33}TiO_3$) were further investigated via XPS. Fig. 3b displays the XPS spectra of Ti. The XPS peak at 464.3, 458.6, 462.9 and 457.1 are attributed to Ti^{4+}(2p3/2 and 2p1/2) and Ti^{3+}(2p3/2 and 2p1/2), respectively [21,22]. It suggests that Ti ions are in a mixed valence, which is beneficial to improve the conductivity [17,21].

In order to evaluate the rate capability of samples, the cells were discharged at different rates from 1 to 30 C rates stepwise. Fig. 4a

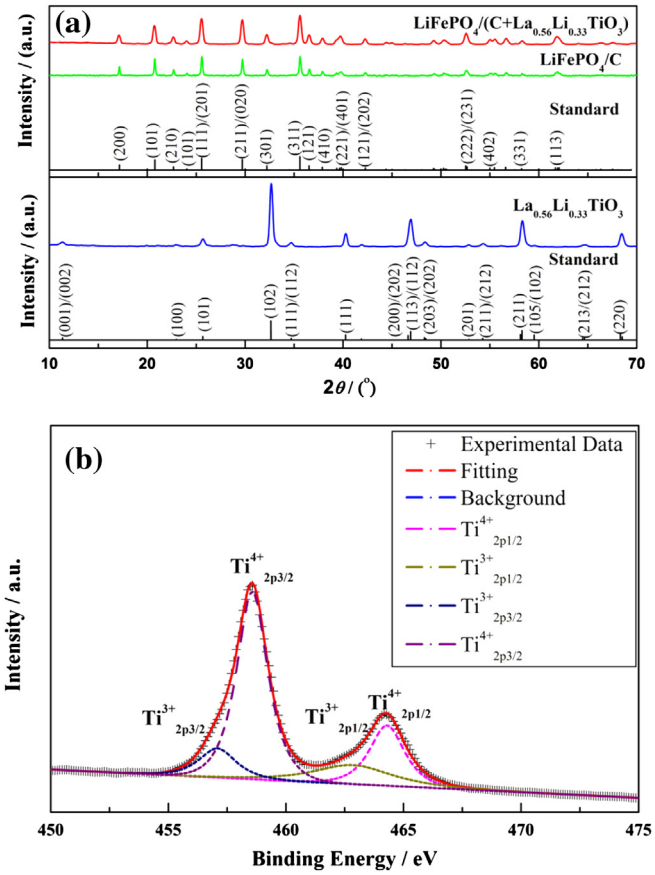

Fig. 3. (a) XRD patterns of the samples; (b) XPS spectra of Ti for synthesized $LiFePO_4$/(C + $La_{0.56}Li_{0.33}TiO_3$).

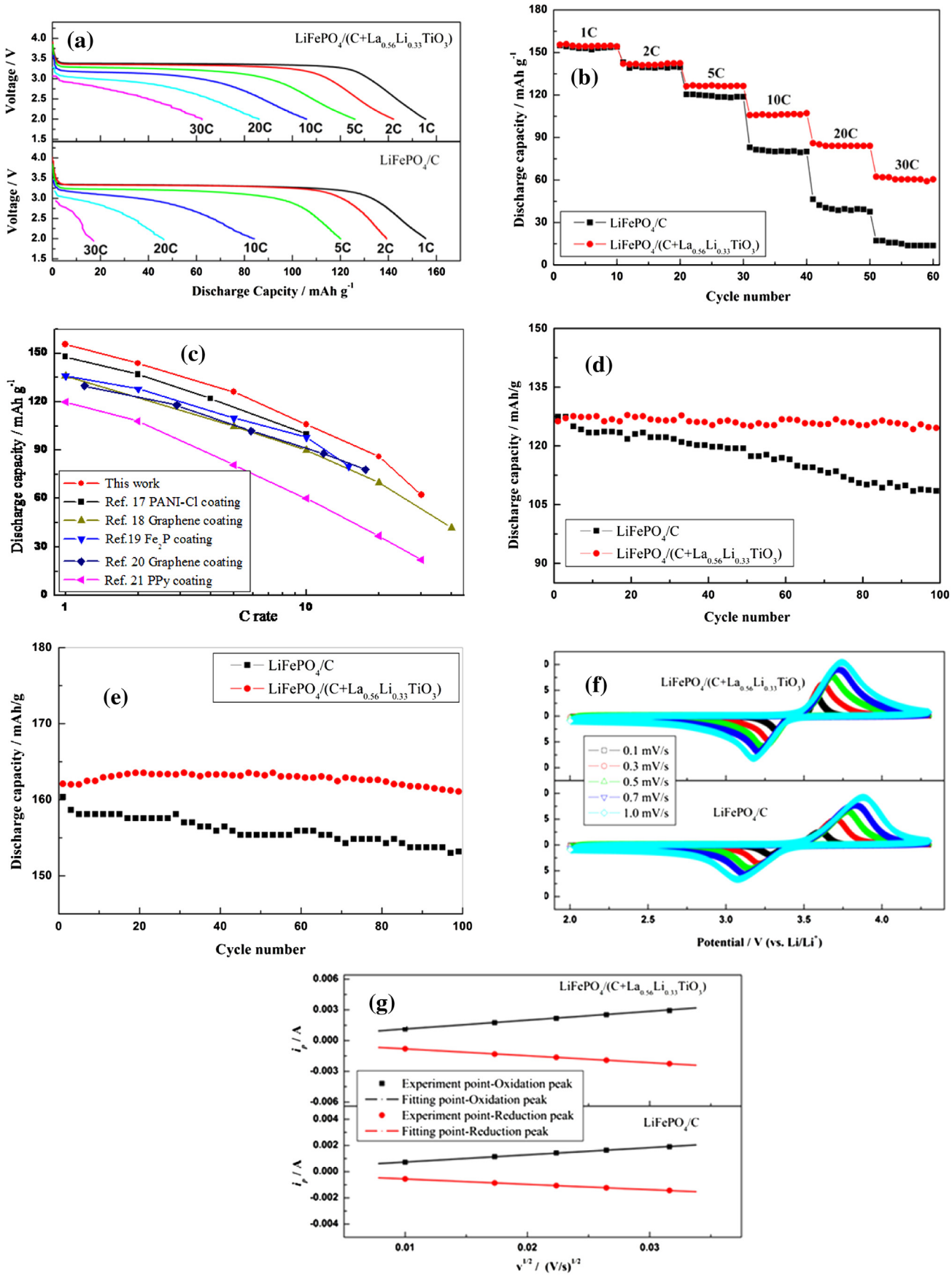

Fig. 4. (a) Discharge curves and (b) cycle performance of the samples at various rates; (c) The rate capacity of $LiFePO_4/(C + La_{0.56}Li_{0.33}TiO_3)$ compared with previous works; The cycle life curves of samples at rates of (d) 5 C at 25 °C and (e) 1 C at 55 °C; (f) Cyclic voltammograms of samples at various scan rates; (g) The curve of peak current (i_p) as a function of square root of scan rate ($v^{1/2}$) of samples.

shows the discharge profiles at 1 C–30 C, the corresponding rate cycling performance is shown in Fig. 4b. The discharging voltage of $LiFePO_4$/C obviously decreases and becomes indistinct with the discharging current increasing to 30 C. While the discharging voltage of $LiFePO_4/(C + La_{0.56}Li_{0.33}TiO_3)$ decreases less than those of $LiFePO_4$/C at 1 C–30 C. As shown in Fig. 4b, compared to $LiFePO_4$/C, $LiFePO_4/(C + La_{0.56}Li_{0.33}TiO_3)$ displays remarkably improved rate capability, especially at higher rates. $LiFePO_4/(C + La_{0.56}Li_{0.33}TiO_3)$ delivers a discharge capacity of 155.5, 142.1, 126.1, 105.8, 86.0 and 62.3 mAh g^{-1} at 1 C–30 C, respectively, higher than those of $LiFePO_4$/C (154.9, 141.0, 120.3, 83.0, 46.5 and 17.2 mAh g^{-1} at 1 C–30 C). These data are significantly higher than the results reported by other groups about double modification $LiFePO_4$ with carbon and other electronic conductive materials, which are listed and compared in Fig. 4c. [23–27]. It is due to both of electronic and Li^+ transport for $LiFePO_4/(C + La_{0.56}Li_{0.33}TiO_3)$ can be enhanced, rather than improving only electronic transferred in the above references via double modification with carbon and other electronic conductive materials.

The cycling performance of samples at 5 C (850 mA g^{-1}) is exhibited in Fig. 4d. It can be seen that $LiFePO_4$/C and $LiFePO_4/(C + La_{0.56}Li_{0.33}TiO_3)$ exhibit the initial discharge capacities of 127.5 and 126.3 mAh g^{-1}, with retention ratios of 84.7% and 99.9% after 100 cycles, respectively. The cycling performance of samples at elevated temperature is further investigated in Fig. 4e. As shown in Fig. 4e, $LiFePO_4$/C and $LiFePO_4/(C + La_{0.56}Li_{0.33}TiO_3)$ deliver the initial discharge capacities of 160.4 and 162.1 mAh g^{-1}, with retention ratios of 95.5% and 99.6% after 100 cycles, respectively. The electrochemical performance of materials is remarkably enhanced, which can be attributed to the enhancement of electronic and Li^+ transport. Moreover, the surface coating layer composed of C and $La_{0.56}Li_{0.33}TiO_3$ could provide an effective protective layer for $LiFePO_4$ core particles to shield them from direct contact with the acidic electrolyte, and thus can deliver excellent cycling performance [2,9–16].

Fig. 4f shows the CV curves of the synthesized samples at a scan rate from 0.1 to 1.0 mV s^{-1}. Each of the CV curves consists of one pair of redox peak at around 3.5 and 3.4 V, corresponding to the charge/discharge reaction of the Fe^{3+}/Fe^{2+} redox couple. Obviously, the intensity and area of the redox peaks enhance with the increase of scan rate. The linear relationship of the peak current (i_p) as a function of square root of scan rate ($v^{1/2}$) is illustrated in Fig. 4g. Thus, the chemical diffusion coefficient can be derived according to the following Randles–Sevcik equation:

$$i_p = \left(2.69 \times 10^5\right) n^{3/2} A D_{Li}^{1/2} C_o v^{1/2} \quad (1)$$

Where, i_p is the peak current, n is the charge transfer number, C_o is the concentration of lithium ions in the cathode, D_{Li} is the chemical diffusion coefficient of Li^+, v is the scan rate and A is the surface area. However, the determination of the actual surface area of active materials is a difficult task due to the presence of C in the $LiFePO_4$/C or $LiFePO_4/(C + La_{0.56}Li_{0.33}TiO_3)$ composites. Namely, classical BET method of surface area measurement may lead to a significantly overestimated value, since carbon surface may be very developed and participate predominantly in the measured value [28]. Here, A is estimated on the basis of equation [29–33]:

$$A = \frac{3m}{r\rho} \quad (2)$$

Where, r is the average particle radius which obtained from SEM image shown in Fig. 2a, ρ is the bulk density. The calculated A via Eq. (2) is around 34.3 cm^2. The corresponding diffusion coefficient of Li^+ can be calculated by Eq. (1) from the slope of i_p vs sqrt(v) in Fig. 4g. During charge/discharge process, the D_{Li} of $LiFePO_4$/C is 1.04×10^{-13} and 5.79×10^{-14} cm^2 s^{-1}, while $LiFePO_4/(C + La_{0.56}Li_{0.33}TiO_3)$ is 6.30×10^{-13} and 4.12×10^{-13} cm^2 s^{-1}, respectively. Apparently, the D_{Li} of $LiFePO_4/(C + La_{0.56}Li_{0.33}TiO_3)$ shows a notable increase compared to that of $LiFePO_4$/C, suggesting that $LiFePO_4/(C + La_{0.56}Li_{0.33}TiO_3)$ is more favourable than $LiFePO_4$/C to lithium ion diffusion.

4. Conclusions

The spherical $LiFePO_4/(C + La_{0.56}Li_{0.33}TiO_3)$ composites have been successfully synthesized by an ammonia assisted hydrothermal method. C and $La_{0.56}Li_{0.33}TiO_3$ are synchronously coated on the surface of spherical $LiFePO_4$. The composites showed an excellent electrochemical performance. It still revealed a high discharge capacity of 62.3 mAh g^{-1} at high rate of 30 C. Therefore, hybrid coating with C and $La_{0.56}Li_{0.33}TiO_3$ is an effective approach to improve the electrochemical performance of $LiFePO_4$ materials. Furthermore, this strategy could be potentially extended to other materials for lithium ion batteries.

Acknowledgements

This work was financially supported by the National Natural Science Foundation of China under project Nos. 20871101, 51272221 and 51302239, the Project of Major Science and Technological Achievement Transformation in Hunan Province No. 2012CK1006 and the Project supported by Science and Technology Department of Hunan Province No. 2012FJ4095.

References

[1] A.K. Padhi, K. Nanjundaswamy, J.B. Goodenough, J. Electrochem. Soc. 144 (1997) 1188.
[2] L.X. Yuan, Z.H. Wang, W.X. Zhang, X.L. Hu, J.T. Chen, Y.H. Huang, Energy Environ. Sci. 4 (2011) 269.
[3] H.C. Shin, K.Y. Chung, W.S. Min, D.J. Byun, Electrochem. Commun. 10 (2008) 536.
[4] C.W. Wang, A.M. Sastry, K.A. Striebel, K. Zagib, J. Electrochem. Soc. 152 (2005) A1001.
[5] F. Yu, J. Zhang, Y. Yang, G.Z. Song, J. Power Sources 189 (2009) 794.
[6] H.B. Shu, X.Y. Wang, Q. Wu, B.W. Ju, L. Liu, J. Electrochem. Soc. 158 (2011) A1448.
[7] H.B. Shu, X.Y. Wang, Q. Wu, L. Liu, Q.Q. Liang, Electrochim. Acta 76 (2012) 120.
[8] H.B. Shu, X.Y. Wang, Q. Wu, Q.Q. Liang, X.K. Yang, J. Electrochem. Soc. 159 (2012) A1904.
[9] C. Miao, P.F. Bai, Q.Q. Jiang, S.Q. Sun, X.Y. Wang, J. Power Sources 246 (2014) 232.
[10] S.P. Wang, H.X. Yang, L.J. Feng, Y.Z. Yang, J. Power Sources 233 (2013) 43.
[11] L. Wang, W.T. Sun, X.Y. Tang, X.K. Huang, X.M. He, J.J. Li, J. Power Sources 244 (2013) 94.
[12] L.F. Cheng, G.X. Liang, S.E. Khakani, D.D. MacNeil, J. Power Sources 242 (2013) 556.
[13] J.P. Jegal, K.B. Kim, J. Power Sources 243 (2013) 859.
[14] W.L. Liu, J.P. Tu, Y.Q. Qiao, J.P. Zhou, S.J. Shi, X.L. Wang, C.D. Gu, J. Power Sources 196 (2011) 7728.
[15] J.Y. Xiang, J.P. Tu, L. Zhang, X.L. Wang, Y. Zhou, Y.Q. Qiao, Y. Lu, J. Power Sources 195 (2010) 8331.
[16] M.M. Rahman, J.Z. Wang, R. Zeng, D. Wexler, H.K. Liu, J. Power Sources 206 (2012) 259.
[17] Y. Inaguma, C. Liquan, M. Itoh, T. Nakamura, Solid State Commun. 86 (1993) 689.
[18] H. Kawai, J. Kuwano, J. Electrochem. Soc. 141 (1994) L78.
[19] Y. Harada, T. Ishigaki, H. Kawai, Solid State Ionics 108 (1998) 407.
[20] M. Abe, K. Uchino, Mater. Res. Bull. 9 (1974) 147.
[21] K.Y. Yang, K.Z. Fung, M.C. Wang, J. Appl. Phys. 100 (2006) 056102.
[22] J.P. Miao, Z. Lü, L.P. Li, F.L. Ning, Z.G. Liu, X.Q. Huang, Y. Sui, Z.N. Qan, W.H. Su, J. Alloys Compd. 387 (2005) 287.
[23] E. Avci, M. Mazman, D. Uzun, E. Bicer, T. Sener, J. Power Sources 240 (2013) 328.
[24] Y. Zhang, W. Wang, P. Li, Y.B. Fu, X.H. Ma, J. Power Sources 210 (2012) 47.
[25] Y.H. Yin, M.X. Gao, H.G. Pan, L.K. Shen, J. Power Sources 199 (2012) 256.
[26] J. Ha, S.K. Park, S.H. Yu, A.H. Jin, B. Jang, S.Y. Bong, I. Kim, Y.E. Sung, Nanoscale 5 (2013) 8647.

[27] C.W. Sun, S.Y. Rajasekhara, J.B. Goodenough, F. Zhou, J. Am. Chem. Soc. 133 (2011) 2132.
[28] C.Z. Lu, G.T.K. Fey, H.M. Kao, J. Power Sources 189 (2009) 155.
[29] M. Vujković, I. Stojković, N. Cvjetićanin, S. Mentus, Electrochimica Acta 92 (2013) 248.
[30] K. Wang, R. Cai, T. Yuan, X. Yu, R. Ran, Z.P. Shao, Electrochimica Acta 54 (2009) 2861.
[31] J. Chong, S.D. Xun, X.Y. Song, P. Ridgway, G. Liu, J. Power Sources 200 (2012) 67.
[32] C.H. Mi, X.G. Zhang, H.L. Li, J. Electroanal. Chem. 602 (2007) 245.
[33] P. He, X. Zhang, Y.G. Wang, L. Cheng, Y.Y. Xia, J. Electrochem. Soc. 155 (2008) A144.